The Effect of Process Parameters on Alignment of Tubular Electrospun Nanofibers for Tissue Regeneration Purposes

Rossella Dorati[1,5], Enrica Chiesa[1], Silvia Pisani[2], Ida Genta[1,5], Tiziana Modena[1,5], Giovanna Bruni[3], Chiara R.M. Brambilla[1], Marco Benazzo[4], Bice Conti[1,5,*]

[1] Department of Drug Sciences and, University pf Pavia, V.le Taramelli 12/14, 27100, Pavia, Italy
[2] Department of Paediatric Oncoaematology IRCCS Policlinico S.Matteo, Pavia, P.zzle Golgi 1, 27100, Pavia, Italy
[3] Department of Chemistry, University pf Pavia, V.le Taramelli 12/14, 27100, Pavia, Italy
[4] Department of Otholaryngology Head Neck Surgery, University of Pavia and IRCCS Policlinico S.Matteo, P.zzle Golgi 1, 27100, Pavia, Italy
[5] Polymerix srl, V.le Taramelli 20, 27100, Pavia, Italy

ARTICLE INFO

ABSTRACT

Electrospinning is known to be an effective and straightforward technique to fabricate polymer non woven matrices made of nano and microfibers. Micro patterned morphology of electrospun matrices results to be outmost advantageous in the biomedical field, since it is able to mimic extracellular matrix (ECM), and favors cell adhesion and proliferation. Controlling electrospun fibers alignment is crucial for the regenerative purposes of certain tissues, such as neuronal and vascular. In this study we investigated the impact of electrospinning process parameters on fiber alignment in tubular nanofibrous matrices made of Poly (ʟ-lactide-co-ε-caprolactone) (PLA-PCL); a Design of Experiments (DoE) approach is here proposed in order to statistically set up the process parameters. The DoE was studied keeping constants the previously set material and environmental parameters; voltage, flow rate and mandrel rotating speed were the process parameters here investigated as variables. Orientation analysis was based on ImageJ and plugin Orientation J analysis of SEM images. The results show that voltage combined with flow rate has significant impact on electrospun fiber orientation, and the greatest orientation is achieved when all the three input parameters (voltage, flow rate and mandrel rotation speed) are at their maximum value.

1. Introduction

Electrospinning is known to be an effective and straightforward technique to fabricate polymer non woven matrices made of nano and microfibers. The technique is based on interfacial phenomena rising when an electric field is applied to a polymer solution. The electric field generates a charge in the polymer solution, and when the electric force overcomes the solution surface tension, a polymeric jet, making a typical Taylor cone, is generated from the surface tension and travels towards the collector [1,2]. Viscosity of the polymer solution and its surface tension are interconnected in the process, since high viscosity stabilizes the forming fiber, while low surface tension promotes its stretching. Electrospun nanofibrous matrix forms due to deposition of entangled polymer fibers on the collector; polymer solvent evaporation is provided along jet pathway between needle and collector.

Electrospinning technique has been applied to several fields such as filtration, electronic and photonic technology [3–6], and it has drawn particular attention in the biomedical area of tissue engineering because the electrospun matrices, made of suitable biodegradable and biocompatible polymers, can be seeded with cells and act as scaffold for tissue regeneration [7–12]. An important advantage of the electrospun matrices is their micro patterned morphology that mimics extracellular matrix (ECM), thus favouring cell adhesion and proliferation. It has been demonstrated in the literature that aligned nanofibers are able to orient cells in the specific direction needed to provide the anisotropy encountered in certain organs including blood vessels, muscular tunic of esophagus, urethra, and in general of any hollow organ or tubular structure, and in tissues such as neuronal tissue [13–18]. Thus, the electrospinning parameters should be profitably adjusted in order to control diameter, alignment of fibers, meanwhile keeping suitable spinnable regimen of the polymer solution.

These parameters can be classified as follows: *i)* process parameters (electric field, polymer solution flow rate, syringe needle gauge, mandrel rotating speed), *ii)* material parameters (polymer solution

---

viscosity, surface tension and ionic conductivity, polymer molecular weight) and *iii)* environmental parameters (relative humidity (RH) and temperature of electrospinnng chamber). Several authors account material parameters to be the most decisive factors for spinnability and uniform shape of the fibers, while environmental parameters are derived thereof [19–21]. Eventually, once fixed the materials and environmental parameters, process parameters can play a significant role in affecting size and alignment of the fibers. The topic drawn interest for several years, and it still is of interest for those scientists working in the area of tissue engineering, as demonstrate the papers found in the literature [22–27].

Although electrohydrodynamic atomization techniques (including electrospinning, electrospraying and e-jetting) are moving forward fast to the multifluid processes for creating complex nanostructures, such as core-shell, tri-layer and side-by-side (Janus) [5,28–30], few attention has been paid to the alignment of their products that hold great potential applications in biomedical fields. Moreover, a series of efforts were aimed to the influence of operational parameters on characteristics of electrospinning, and even ambient conditions on the resultant nanofibers' quality [29,31,32] but few publications have been reported on the relationship between the working parameters and the alignment effect of electrospun nanofibers.

Starting from this background, the work was aimed to study electrospinning process parameters through a quality by design approach. A Design of Experiments (DoE) was set up in order to statistically evaluate which electrospinnig process parameters affect nanofiber alignment in electrospun tubular matrices made of Poly (L-lactide-co-ε-caprolactone) (PLA-PCL).

PLA-PCL was selected because it is a biodegradable and biocompatible polymer whose properties, such as long biodegradation time and elasticity, make it suitable for application in regeneration of blood vessels and other hollow tubular human organs. The copolymer can also be used in combination with other biodegradable polymers such as Polylactide or Polylactide-co-glycolide. Indeed, a lot of studies in the literature characterize these last polymers, while less investigation has been performed on PLA-PCL copolymer, highlighting there is room for studies on PLA-PCL addressed to regeneration purposes [27,33–35].

Quality by design approach is an important consolidated tool in pharmaceutical industry, and it was applied to electrospinning process with interesting results towards different variables and diverse polymers [36,37]. DoE has been chosen and used in this work because it is a systematic method to determine the relationship between variables affecting a process and the output of that process. It is a statistical driven powerful data collection and analysis tool that has been recognized useful in order to set up and optimize process parameters [35].

Data processing: ImageJ software was used in this work to measure the orientation distribution function of the fibers in a plane environment. This post processing technique is based on digital imaging and takes advantages of using algorithm method to measure fiber orientation. The technique finds consolidated application more in general with quality target product design and more specifically for fiber alignment evaluation in particular in electrospinning [38–40].

The investigated electrospun matrices are intended for tissue engineering applications, namely vascular grafts or esophagus reconstruction, for this reason in this work attention was focused on a biodegradable biocompatible polymer already approved by FDA for use in the human body.

2. Materials and methods

2.1. Materials

Poly (L-lactide-co-ε-caprolactone) 70:30, Mw 160241 Da (PLA-PCL, RESOMER LC 703 S) was from Evonik Industries (Evonik Nutrition & Care GmbH, 64275 Damstadt, Germany). Methylen chloride (MC) 99,9% purity and N,N-Dimethylformammide (DMF) 99,8% purity were from Carlo Erba (Carlo Erba SpA, Milano, Italia).

2.2. Methods

2.2.1. Material parameters: selection of polymer solvent and polymers ratio/concentration

The solvents used in electrospinning process should have low boiling points, in order to evaporate on the way to the electrospinning collector, and high dielectric constant in order to promote fiber stretching. PLA-PCL is soluble in several organic solvents such as methylene chloride, chloroform, carbon tetrachloride, dimethylformamide, tetrahydrofuran. The solvents selected to solubilize PLA-PCL were Methylene chloride (MC) and Dimethylformamide (DMF). MC was chosen because, is the one showing the lowest boiling point, i.e. 40 °C, among the polymer solvents. However, its dielectric constant is 8.93, very low, and mixing with DMF, whose dielectric constant is 36.7, although its high boiling point is 153 °C, permits to rise the dielectric constant of polymer solution, improving nanofiber formation process. The properties of the selected polymer solvents, to be considered for electrospinning process, are summarized in Table 1.

Polymer concentration in the solvent mixture, and the solvents ratio was determined by evaluating the crossover point between surface tension and viscosity curves of the copolymer solutions at fixed concentration and different solvent ratios. According to the literature [26] this corresponds to the best condition for electrospinning, since it is the point of lowest surface tension and highest viscosity (namely high viscosity stabilizes the forming fiber and low surface tension favors its stretching).

Surface tension of PLA-PCL 10% and 15% w/v solutions in the solvent mixtures of MC:DMF 60:40, 70:30, 75:25, 80:20 v/v ratios, were measured by Du Nouy's tensiometer with a manual force tensiometer K6 (KRÜSS GmbH – Hamburg, Germany). The method involves slowly lifting a platinum ring from the surface of a liquid. The force required to raise the ring from the liquid's surface is directly proportional to its surface tension (γ) according to the following Equation (1):

$$\gamma = \frac{F \times k}{2 \times \Phi} \qquad \text{(Eq. 1)}$$

where F is the force, k is the correction factor and Φ is the ring's circonference. Each measure performed in triplicate, the results are reported as mean ± standard deviation.

Viscosity values of the PLA-PCL solutions at 10% and 15% w/v in solvent mixtures of MC:DMF 60:40, 70:30, 75:25, 80:20 v/v ratios were measured by Rheometer Kinexus Pro Malvern (Alfa Test, Cinisello

Table 1
Properties of the polymer solvents (Boiling point, Viscosity, Electric conductivity, Dielectric constant and Surface tension) selected for electrospinning process.

SOLVENTS	Boiling point (°C)	Viscosity (mPa·s)	Electric conductivity (mho)	Dielectric constant	Surface tension (Dyne/cm)
Methylene chloride (MC)*	39.7	0.410	4.3×10^{-11}	10.7	28.20
(N,N) -Dimethylformamide (DMF)*	153	0.802	6.0×10^{-2}	36.70	36.42

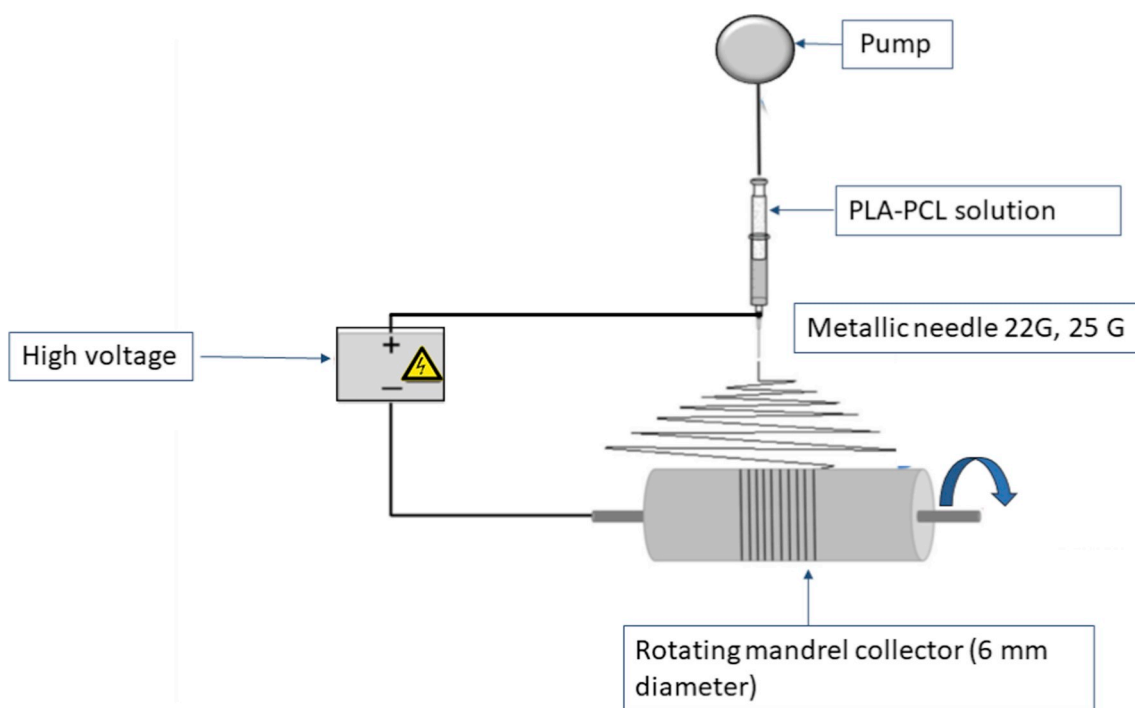*Data from PubChem and Dow Chemical Company product information.

Fig. 1. Scheme of basic electrospinning set up equipped with pump, high voltage supply and rotating mandrel collector.

Balsamo, Italy) with cone-plate geometry, constant share rate 100 s^{-1}, 25 °C and solvent trap. The share rate value was chosen because it simulates the one that develops inside electrospinning apparatus during ejection process. Each measure performed in triplicate, the results are reported as mean ± standard deviation.

2.2.2. Electrospinning of PLA-PCL

Electrospinning apparatus Nanon-01A (MECC Instruments, Ltd, Ogo-shi, Fukuoka, Japan) equipped with a dehumidifier system (196-1 Fukudo Ogori-Shi, Japan) was used. Electrospinning process schematized in Fig. 1 works as follows. Polymer solution is loaded in a 5 mLLuer lock plastic syringe (Luer lock syringe, DB) and it is pumped through the syringe needle, across an electric field generated by application of high voltage between the syringe needle (primary electrode) and the collector (counter electrode). The electrospinning spinneret set is vertical and moves with 50 mm/s fixed speed, a rotating mandrel was chosen as collector, whose diameter was 6.0 mm, and 46.5 cm^2 surface area. The gap between nozzle and the rotating mandrel collector was maintained at 15 cm. Fiber deposition is driven by both electric field and mandrel rotation, this latter developing a centripetal force on fibers. Electrospinning time was 15 min for all samples. This time was chosen because it allows to form entangled matrices that completely coats the rotating mandrel surface independently of rotating mandrel speed. The electrospinning time was fixed and it was not considered a variable, as long as electrospinning temperature and relative humidity (RH%) that were 25 °C and 40% respectively.

2.2.3. Design of experiment (DoE)

A DoE full factorial experimental design was applied, applied voltage (kV), mandrel rotating speed (rad/sec) and polymer solution flow rate (mL/h) were the input variables (process parameters), and fiber orientation was the output parameter analysed as summarized in Table 2. The design matrix for the evaluated variables took into account all possible combinations of maximum and minimum values for each input variable, as reported in Table 3. Maximum value was defined +1 and minimum value −1, intermediate value 0. Number of possible combinations depends on number of input variables considered and was 2^n, where n corresponded to the number of input variables

Table 2
DoE matrix set up.

Number of input variables	3
Number of output parameters	1
Number of runs	9, including one central point per block
Degree of freedom	2
Randomized	Yes

Table 3
Minimum, maximum and intermediate values of set input parameters.

	Minimum value (−1)	Intermediate value (0)	Maximum value (+1)
Voltage (kV)	22	26	30
Flow rate (mL/h)	1	3	5
Mandrel rotation speed (rad/sec)	104.72	183.26	261.80

Table 4
Screening design matrix of the 9 possible combinations of the 3 input variables considered.

Voltage (kV)	Flow rate (mL/h)	Mandrel rotating speed (rad/sec)
+1	+1	+1
+1	+1	−1
−1	+1	+1
+1	−1	+1
−1	+1	−1
+1	−1	−1
−1	−1	+1
−1	−1	−1
0	0	0

evaluated. Table 4 reports the design matrix of the 9 possible combinations of the 3 input variables considered in this work.

The experiments were executed in random order as protection against dormant variables; two degree of freedom were available to evaluate the experimental error. Response surface analysis was applied

Table 5
DoE design matrix derived from the values in Tables 3 and 4.

Batch n. (run number)	Voltage (kV)	Flow rate (mL/h)	Mandrel rotation speed (rad/sec)
1	30 (+1)	5 (+1)	261.80 (+1)
2	30 (+1)	1(-1)	261.80 (+1)
3	22 (−1)	5 (+1)	261.80 (+1)
4	30 (+1)	5 (+1)	104.72 (−1)
5	22 (−1)	1 (−1)	261.80 (+1)
6	30 (+1)	1(-1)	104.72 (−1)
7	22 (−1)	5 (+1)	104.72 (−1)
8	22 (−1)	1 (−1)	104.72 (−1)
9	26 (0)	3 (0)	183.26 (0)

as optimization technique, where the response of a series of full factorial experiments was mapped to generate mathematical equations that describe how the factors affect response. Materials parameters, i.e. PLA-PCL solution concentration and solvent mixture composition were set following the results of preliminary evaluation on surface tension and rheology measurements, and they were not considered input variables of DoE.

Starting from the matrix reported in Table 4, preliminary electrospinning tests were carried out in order to select which could be the highest and the lowest value of each parameter achieving a stable polymer jet in the electrospinning process, i.e. able to generate a Taylor cone. Please note that the maximum voltage value corresponded to the maximum value allowed by the apparatus specifications. The values of set input parameters derived from these preliminary tests are listed in Table 3, and the consistently built design matrix is reported in Table 5.

Input and output factors were statistically processed by Statgraphics XVIII software (ANOVA, regression coefficient R^2), in order to avoid false positive and to get statistically significant results. Voltage was set up as Factor A, flow rate was Factor B and mandrel rotation speed was Factor C. The effect of the 3 factors was evaluate in 9 runs according to the matrix reported in Table 5. Experiments execution was completely randomized in order to protect from effect of dormant variables. Only 2° of freedom were involved in the evaluation of experimental error.

2.2.4. Characterization of the electrospun nanofibrous matrices

All electrospun samples were analysed by Scanning Electron Microscopy (SEM) with a Zeiss EVO MA10 apparatus (Carl Zeiss, Oberkochen, Germany). All samples were dried and gold sputtered before undergo SEM analysis.

Morphometric analysis of the electrospun nanofibers was quantitatively performed processing SEM images by ImageJ software. This is an image processing program designed for scientific multidimensional images and based on plugin series Diameter J Segment e Diameter J 1–018.

Diameter J Segment plugin algorithm works by segmenting SEM image and allows selection of images. Selected segmented image/or images to best represent a sample should have the following characteristics: absence of partial fibers, fiber intersection shouldn't contains black spots/hole. When two or more images of the sample are very similar, best choice should be the one containing highest number of fibers. Super Pixel is the plugin that calculate mean fibers' diameter, using a super pixel determination (the scale length set was 202 pixels for 1 cm). Mean fibers' diameter was determined by Histogram Mean, fitting a Gaussian Curve to the radius data and finding the curves mean value. Histogram SD, delineates the standard deviation of the Gaussian fit of the radius histogram. Histogram Mode and Histogram Median determine the most occurring fiber diameter in the histogram and the middle fiber diameter respectively. Histogram Min. Diam. and Histogram Max. Diam define the smallest and the largest diameter measured. Histogram Integrated Density calculates the product of length of the fibers and the average radius, then Histogram Raw Integrated Density determines the sum of the radii at all pixels in the image or selection. Diameter Skewness measures the third order moment about the mean; Diameter Kurtosis the fourth. All the data obtained from Image processing analysis were then plotted by using Microsoft Excel.

The values of orientation were obtained analyzing SEM images with ImageJ and plugin Orientation J software, that analysed the degree of fiber orientation distribution from −90° to +90°, of each SEM image using Fast Fourier transform (0° angle corresponded to the horizontal orientation parallel to mandrel axis and increased counter-clockwise). Analysis was performed on 6 SEM images for each electrospun matrix sample.

Yield of process was determined for each sample from the following equation 2

$$Yield\ of\ process = \frac{Ws}{Wi} \times 100 \tag{Eq.2}$$

Where W_s is the sample weight and W_i is the amount of polymer in the starting polymer solution, and it is calculated following equation (3):

$$Wi = \frac{15g}{100\ mL} \times mL\ of\ electrospun\ solution\ making\ a\ sample \tag{Eq.3}$$

Samples were prepared in triplicate and yield process variability evaluated in terms of mean ± standard deviation (sd).
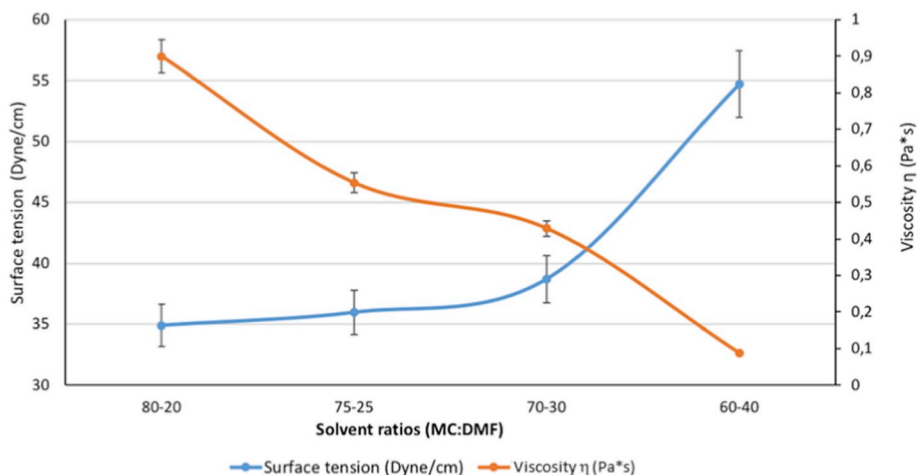
Fig. 2. Surface tension and viscosity curves of PLA-PCL 15 % w/v as a function of different MC:DMF ratios.

3. Results

The results of preliminary evaluation, carried out to set up the material parameters, are reported in Fig. 2 and show that PLA-PCL 15% w/v solution increases its surface tension as long as DMF content increases, while viscosity decreases in the same conditions. The crossover point of the two curves resides between 70:30 and 60:40 solvent ratios. Similar result was obtained for PLA-PCL 10% w/v solution (curves not reported). Considering this result, two intermediate solvent ratios, 65:35 and 68:32, were selected and the PLA-PCL solutions were electrospun at 261.80 rad/s mandrel rotation speed. The preliminary set of tests were carried out in order to select and fix material parameters i.e. PLA-PCL concentration in the starting solution and one solvent ratio between those that could be suitable. The results of SEM analyses (data not reported) showed that electrospinning of PLA-PCL 10% w/v solutions did not reach satisfactory results independently of MC-DMF ratios tested; the fibers did not form regularly and some of them were melted together originating irregular cluster inside the matrix. Electrospinning of PLA-PCL 15% w/v solutions gave better results in terms of regular fibers formation originating a network with homogeneous structure. Starting from these results only electrospun matrices obtained from PLA-PCL 15% were prepared and processed further.

SEM images referred to electrospun matrix obtained starting from 15% w/v PLA-PCL solutions in 65:35 and 68:32 MC-DMF blends, were processed by software ImageJ, and mean fiber diameter, rank of fiber diameter porosity percentage, mean and standard deviation of pore area were determined. The results reported in Table 6 highlight that mean diameter of electrospun fibers is significantly smaller (0.314 μm with respect to 0.551 μm), and with narrower range of fiber diameter (0.0394–0.6299 μm with respect to 0.0394–1.1024 μm), when the solvent mixture MC:DMF 65:35% v/v was used. However, the samples obtained from 65:35 MC:DMF solution show lower porosity percentage and mean pore area with respect to samples obtained from 68:32 v/v MC:DMF solution (38.08% with respect to 49.56%, and 0.4020 ± 0.484 μm^2 with respect to 0.9492 ± 2.124 μm^2 respectively). Moreover, the matrices obtained from 65:35 MC:DMF solution are more reproducible in these parameters, with lower standard deviation.

These results led to select 65:35 v/v MC:DMF solvent ratio as the composition giving the most consistent results.

The results of input and output variables processed by Statgraphics XVIII ANOVA in order to analyze which variable or couple of variables mostly affect fiber orientation, are reported in Table 7.

ANOVA Table (Table 7) splits out orientation variability for each effect (made of couple of variables) and verifies the statistic significance of each effect by comparing the square mean with an evaluation of experimental error.

R-squared (R^2) analysis indicated that the adjusted model fits 98.1758% of variability in orientation. R^2 adjusted to degree of freedom, that better compares models with independent variables and different numbers, resulted to be 92.703%. R^2 adjusted and R^2 adjusted to degree of freedom resulted of same rank order and confirmed the dependent variable is well explained by the independent variables and that the model was statistically significant. The standard error of the estimated (residual standard deviation) was 766.729; mean absolute error (MAE) was 284.55 and corresponded to residues mean value.

Based on the regression coefficients derived, the following second degree equation (Eq. (4)) was applied to evaluate how each input variable or couple of input variables (Table 7) affected electrospun fiber orientation.

$$\textbf{Fiber Orientation} = 42263.2 - 1440.07 \times \textbf{A} - 7657.09 \times \textbf{B}$$
$$- 8.8776 \times \textbf{C} + 256.573 \times \textbf{A} \times \textbf{B}$$
$$+ 0.312806 \times \textbf{A} \times \textbf{C} + 0.718373 \times \textbf{B} \times \textbf{C}$$

$$\text{(Eq.4)}$$

When the result of equation (4) is a positive value it indicates orientation of electrospun fiber, whereas a negative result indicates lack of fiber orientation. Each number multiplied for the value of each variable or couple of variables, indicates how each variable, or variables interaction, affect fiber orientation. A greater value corresponds to stronger effect, and a lower value to a weaker one.

The results of Table 7 and Fig. 3 show that only AB effect (voltage and flow rate) significantly affected electrospun fibers orientation with P-value lower than 0.05 indicating that this effect significantly differs from 0 with a level of confidence of 95.0%.

Moreover, Pareto chart in Fig. 3 clearly show that: each single input variable is not able to significantly affect fiber orientation; voltage is the input variable with lower effect on electrospun fiber orientation; only the combination of input variables voltage (A) and flow rate (B) significantly affects electrospun fiber orientation.

The effect of each single input variable and of their interactions was decomposed and analysed in the charts reported in Fig. 4.
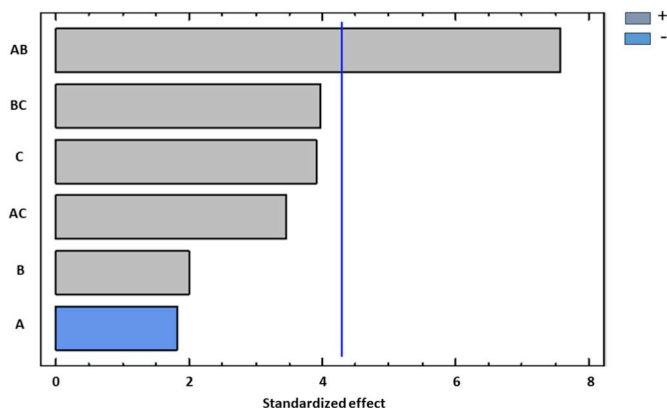
Fig. 4A shows that electrospun fiber orientation is promoted by low voltage (20 kV), high flow rates (up to 5 mL/h) and high mandrel rotation speeds (261.80 rad/s).

As long as the interaction between input variables is concerned, three input variables combination (AB, AC, BC) were investigated and the results in Fig. 4B confirm that main interaction is voltage/flow rate (AB) that significantly affects fiber orientation degree (Fig. 3). High voltage should be combined with low flow rate and vice versa, in order to achieve high orientation degree. AC interaction show that high mandrel rotation speed always favors high orientation degree, independently from the voltage applied. BC interaction indicates that either low or high mandrel rotation speed can be combined to low flow rates in order to get high fiber orientation, whereas in case of high flow rates, high mandrel rotation speed should be applied for achieving better fiber orientation.

The results of electrospun fiber orientation obtained from ImageJ plugin Orientation J analysis of SEM images are reported in Fig. 5 for the batches 1 and 8 that demonstrated the highest degree of the electrospun fiber orientation. Circular color map coding in Fig. 5A gives qualitative indication of fiber orientation, and colors in the processed SEM images of Fig. 5B and C highlighted prevalence of +90° orientation degree (fuchsia color). The traces of orientation (Fig. 5D and E) built taking into account the pixels that have a coherency larger than min-coherency (5%) and an energy larger than min-energy (5%), quantitatively correlate orientation degree with distribution intensity calculated for each image single pixel and give more quantitative information on fiber orientation [41]. The results in Fig. 5D and E showed peaks of preferred orientation at about +60° for batch 1 and about +70° for batch 8. The original SEM images are reported in supplementary data (Fig. S1).

Table 6
Results in terms of fiber diameter and porosity obtained by software ImageJ, plugin Diameter J and plugin Diameter J 1–018.

Sample composition	Mean fibre diameter (μm)	Range of fiber size (μm)	Porosity percentage (%)	Mean pore area $\pm$ sd (μm^2)
PLA-PCL 15%w/v 65:35 MC:DMF	0.315	0.039–0.630	38.08	0.402 ± 0.484
PLA-PCL 15%w/v 68:32 MC:DMF	0.551	0.039–1.102	49.56	0.949 ± 2.124

Table 7

Analysis of variance (ANOVA) on the three input variables (A, B, C) *vs* orientation (output variable).

Nomenclature	Square sum	Degree of freedom	Square mean	F ratio	P-value
Input variable, A: voltage	1.9345×10^6	1	1.9345×10^6	3.29	0.2113
Input variable, B: flow rate	2.34943×10^6	1	2.34943×10^6	4.00	0.1836
Input variable, C: mandrel rotation speed	8.95266×10^6	1	8.95266×10^6	15.23	0.0598
Effect AB	3.37049×10^7	1	3.37049×10^7	57.33	0.0170
Effect AC	7.04504×10^6	1	7.04504×10^6	11.98	0.0743
Effect BC	9.28908×10^6	1	9.28908×10^6	15.80	0.0578
Total error	1.17575×10^6	2			
Total (corrected)	6.44513×10^7	8			

Fig. 3. Pareto chart: influence of the input variables and combination of input variables on electrospun fiber orientation; A voltage, B flow rate, C mandrel rotation speed.

The results confirmed those obtained by DoE statistical analysis. Mandrel rotation speed demonstrated to be a crucial factor to fiber alignment, but the combination of the three input variables also plays a significant role in fiber alignment when electrospinning PLA-PCL copolymer.

The same 9 runs data were analysed and processed by ImageJ software plugins Diameter J 1–018. The results in Table 8 showed significantly smaller fiber size for batches 5, 6, 7 that was neither correlated to porosity % or mean pore area, the latter resulting in high variability. These batches did not show fiber alignment, whereas batches n.1 and 8, showing best fiber alignment resulted in higher fiber diameter size. As long as porosity is concerned the parameter was always greater than 40% with the exception of batches 2, 6 and 8. The result for batches 2 and 6 seems to be related to high voltage (30 kV) and low flow rate (1 mL/h).

Process yield was always lower than 64% (Table 8), and it did not result to be related to electrospun fiber orientation. The result represents a drawback of the electrospinning process that should be further studied and optimized.

4. Discussion

DoE resulted to be an efficient tool to statistically evaluate which electrospinnig process parameters affect nanofiber alignment in electrospinning tubular matrices made of PLA-PCL. Since DoE is widely applied in the pharmaceutical industry, this work corroborates its effectiveness in pharmaceutical applications of electrospinning technique.

Several authors highlight the importance of porosity and mean pore area when considering electrospun matrices for tissue engineering purposes. Porous fibers permit nutrient transport and cell metabolic waste removal therefore improving cell attachment. Electrospinning process *per se* does not create highly porous fibers and for this reason authors tried to improve electrospun fiber porosity through treatments such as ultrasonication, or by modifying the process with an on purpose created 3D collector [42–44]. The present work more was focused on fiber alignment than on creating highly porous fibers, however the electrospun fiber porosity resulted to be always higher than 40% with the exception of three batches whose porosity was <40% but >30%. Porosity seemed to be related to voltage and flow rate and no correlation among fibers orientation, porosity and mean pore area was highlighted.

As long as fiber alignment is concerned, most of the results of other authors reported in the literature are in keeping with the influence of mandrel rotating speed on fiber alignment. whereas the highest fiber orientation degree corresponded to the highest fiber diameter size. Indeed, these results are in keeping with those of other authors such as H.Wang ad coll [15] who performed wet electrospinning process parameters evaluation on high amylose maize starch (HAMS), and Choi and coll [4]. who evaluated electrospinning parameters on poly(ε-caprolactone)/collagen.
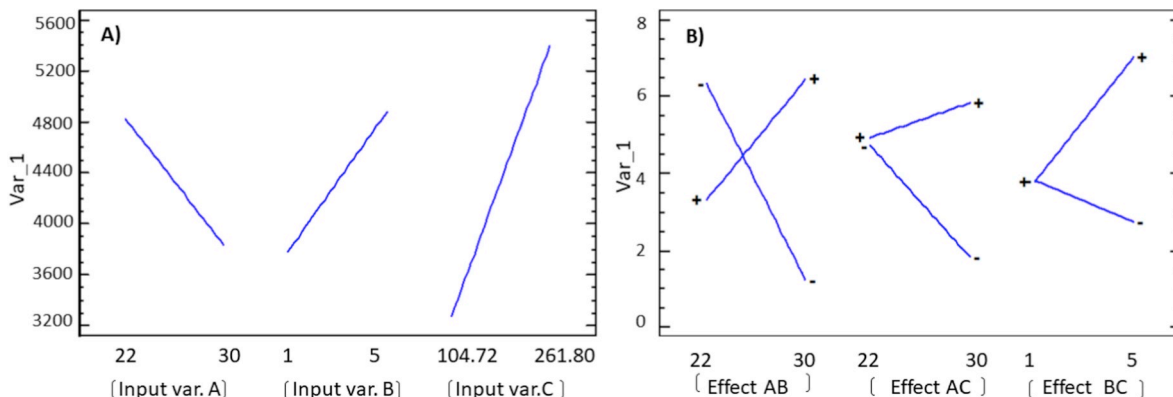
Fig. 4. Graphical representation of DoE results: A) effect of the single input variable on electrospun fiber orientation (output variable); B) Effect of input variables interactions on output variable.
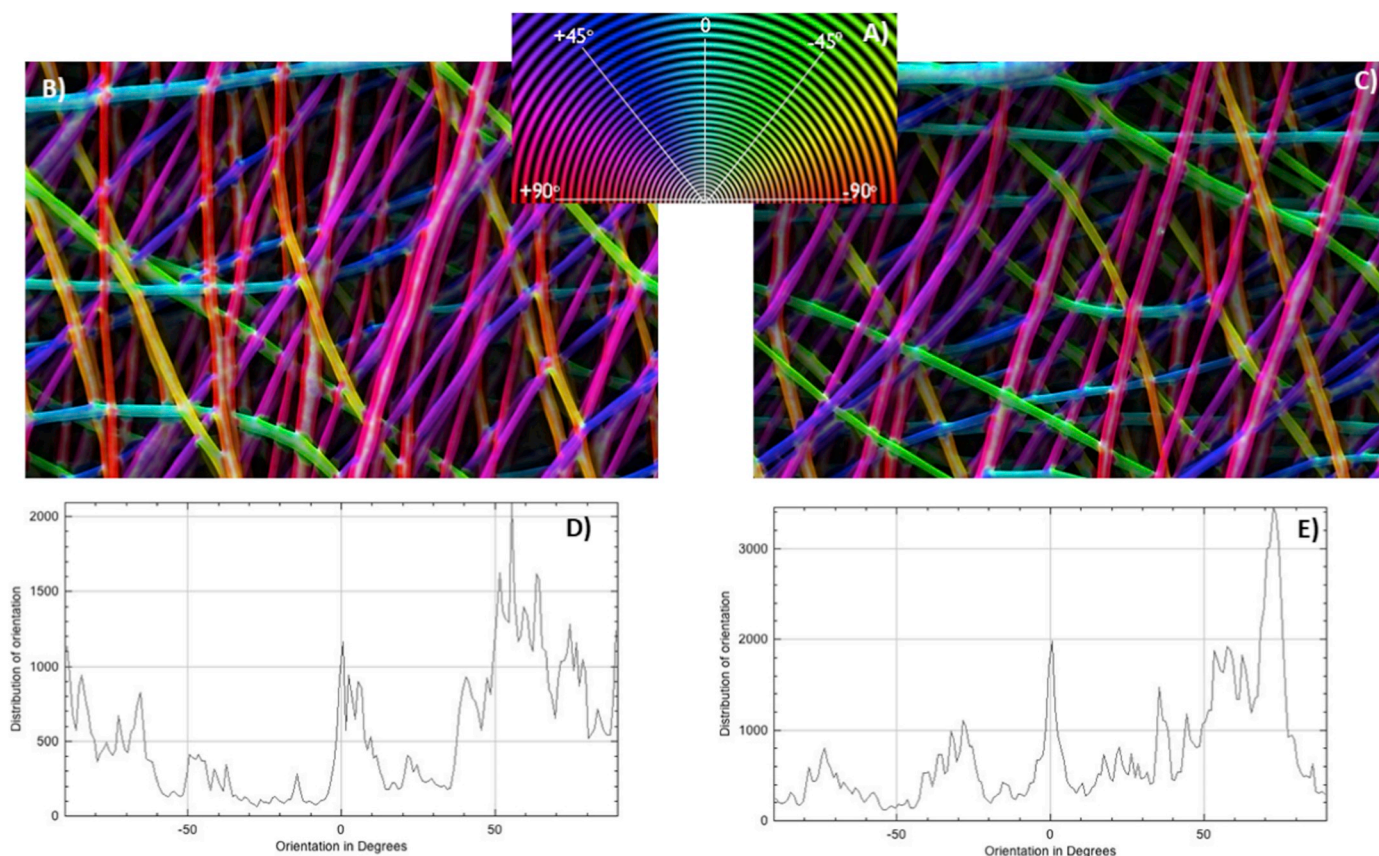
Fig. 5. ImageJ Orientation results: A) circular color map coding; B) color map image of batch 1; C) color map image of batch 8; D) trace of orientation of batch 1; E) trace of orientation of batch 8.

Table 8
Results of Electrospun fibers characterization by ImageJ, plugin Diameter J 1–018 and plugin Orientation J software on the 9 batches obtained in the conditions selected from DoE design matrix.

Batch n.	Mean fiber diameter (µm ± sd)	Porosity %	Mean pore area (µm² ± sd)	Process yield (%)
1	0.590 ± 0.118	47.56	1.8738 ± 3.508	55.68
2	0.413 ± 0.082	36.04	0.7651 ± 2.774	57.33
3	0.511 ± 0.102	40.20	1.7254 ± 3.756	55.52
4	0.492 ± 0.098	43.81	2.4967 ± 8.146	58.61
5	0.374 ± 0.074	41.60	0.9931 ± 1.640	47.73
6	0.315 ± 0.063	32.64	0.4764 ± 0.530	63.47
7	0.374 ± 0.078	46.60	1.3462 ± 2.270	52.64
8	0.433 ± 0.086	36.12	0.9047 ± 1.025	62.67
9	0.492 ± 0.098	45.95	1.6908 ± 2.624	56.62

Anyway, these results shouldn't be considered predictable or obvious because it should be taken into account that set up of mandrel rotation speed depends on type of electrospinning apparatus, namely horizontal or vertical electrospinning, and type of collector, in addition to the type of polymer and solvents used [45,46]. In the same way, an additional component, such as a surfactant or a drug, can change the material properties of the solution to be electrospun, and consequently it can affect the electrospinning process parameters. Therefore, even if the topic of electrospinning aligned fiber has been already investigated, and examples can be found in the literature, it is important to collect studies on this topic with diverse polymers, combination of polymers, drugs and additives. Since the results obtained considered constant material parameters, i.e. polymer and solvents composition, they could be translated and compared within the same class polyester polymers. However, manufacturing of tubular scaffolds made from polyesters is still a challenging topic in tissue engineering when considering neuronal esophageal or vascular tissue regeneration purposes [47–49].

5. Conclusion

In this study PLA-PCL electrospun fiber alignment was studied by means of a DoE approach. The aim of the work was to disclose a process (working parameters)-structure (alignment of fibers) relationship. On the basis of the results obtained it can be said that the process parameters alone can control a certain degree of fibre alignment without adding any additional equipment to electrospinning apparatus.

CRediT authorship contribution statement

Rossella Dorati: Conceptualization. **Enrica Chiesa:** Validation. **Silvia Pisani:** Investigation. **Ida Genta:** Supervision. **Tiziana Modena:** Funding acquisition. **Giovanna Bruni:** Formal analysis. **Chiara R.M. Brambilla:** Formal analysis. **Marco Benazzo:** Funding acquisition. **Bice Conti:** Supervision, Writing - original draft, Writing - review & editing.

Declaration of competing interest

The authors report no conflict of interest. The authors alone are responsible for the content and writing of this article.

Acknowledgements

Appendix A. Supplementary data

Supplementary data to this article can be found online at https://doi.org/10.1016/j.jddst.2020.101781.

References

[1] A. Cisquella-Serra, M. Magnani, Á. Gual-Mosegui, S. Holmberg, M. Madou, M. Gamero-Castaño, Study of the electrostatic jet initiation in near-field electro-spinning, J. Colloid Interface Sci. 543 (2019) 106–113.

[2] S. Liu, D.H. Reneker, Droplet-jet shape parameters predict electrospun polymer nanofiber diameter, Polymer 168 (2019) 155–158.

[3] J. Xue, T. Wu, Y. Dai, Y. Xia, Electrospinning and electrospun nanofibers: methods, materials, and applications, Chem. Rev. 119 (2019) 5298–5415.

[4] J.S. Choi, S.J. Lee, G.J. Christ, A. Atala, J.J. Yoo, The influence of electrospun aligned poly(epsilon-caprolactone)/collagen nanofiber meshes on the formation of self-aligned skeletal muscle myotubes, Biomaterials 29 (2008) 2899–2906.

[5] M. Wang, K. Wang, Y. Yang, Y. Liu, D.G. Yu, Electrospun environment remediation nanofibers using unspinnable liquids as the sheath fluids: a review, Polymers (Basel) (2020) 12.

[6] K. Javed, M. Oolo, N. Savest, A. Krumme, A review on graphene-based electrospun conductive nanofibers, supercapacitors, anodes, and cathodes for lithium-ion batteries, Crit. Rev. Solid State Mater. Sci. 44 (2019) 427–443.

[7] B. Bochicchio, K. Barbaro, A. De Bonis, J.V. Rau, A. Pepe, Electrospun poly(d,l-lactide)/gelatin/glass-ceramics tricomponent nanofibrous scaffold for bone tissue engineering, J. Biomed. Mater. Res. 108 (2020) 1064–1076.

[8] M.A. Teixeira, M.T.P. Amorim, H.P. Felgueiras, Poly(Vinyl alcohol)-based nanofibrous electrospun scaffolds for tissue engineering applications, Polymers 12 (2019) 7.

[9] A. Keirouz, M. Zakharova, J. Kwon, C. Robert, V. Koutsos, A. Callanan, X. Chen, G. Fortunato, N. Radacsi, High-throughput production of silk fibroin-based electrospun fibers as biomaterial for skin tissue engineering applications, Mater. Sci. Eng. C (2020) 110939.

[10] X. Li, L. Huang, L. Li, Y. Tang, Q. Liu, H. Xie, J. Tian, S. Zhou, G. Tang, Biomimetic dual-oriented/bilayered electrospun scaffold for vascular tissue engineering, J. Biomater. Sci. Polym. Ed. 31 (2020) 439–455.

[11] F. Berton, D. Porrelli, R. Di Lenarda, G. Turco, A critical review on the production of electrospun nanofibres for guided bone regeneration in oral surgery, Nanomaterials (Basel) (2019) 10.

[12] S. Pisani, I. Genta, R. Dorati, P. Kavatzikidou, D. Angelaki, A. Manousaki, K. Karali, A. Ranella, E. Stratakis, B. Conti, Biocompatible polymeric electrospun matrices: micro–nanotopography effect on cell behavior, J. Appl. Polym. Sci. (2020) 49223 n/a.

[13] J.S. Choi, S.J. Lee, G.J. Christ, A. Atala, J.J. Yoo, The influence of electrospun aligned poly(ε-caprolactone)/collagen nanofiber meshes on the formation of self-aligned skeletal muscle myotubes, Biomaterials 29 (2008) 2899–2906.

[14] K.H. Patel, A.J. Dunn, M. Talovic, G.J. Haas, M. Marcinczyk, H. Elmashhady, E.G. Kalaf, S.A. Sell, K. Garg, Aligned nanofibers of decellularized muscle ECM support myogenic activity in primary satellite cells in vitro, Biomed. Mater. 14 (2019) 035010Bristol, England.

[15] L. Wang, Y. Wu, T. Hu, P.X. Ma, B. Guo, Aligned conductive core-shell biomimetic scaffolds based on nanofiber yarns/hydrogel for enhanced 3D neurite outgrowth alignment and elongation, Acta Biomater. 96 (2019) 175–187.

[16] C. Zhang, X. Wang, E. Zhang, L. Yang, H. Yuan, W. Tu, H. Zhang, Z. Yin, W. Shen, X. Chen, Y. Zhang, H. Ouyang, An epigenetic bioactive composite scaffold with well-aligned nanofibers for functional tendon tissue engineering, Acta Biomater. 66 (2018) 141–156.

[17] J. Xue, T. Wu, Y. Xia, Perspective: aligned arrays of electrospun nanofibers for directing cell migration, Apl. Mater. 6 (2018) 120902.

[18] H. Xia, Y. Xia, An in vitro study of non-aligned or aligned electrospun poly(methyl methacrylate) nanofibers as primary rat astrocytes-loading scaffold, Mater. Sci. C Mater. Biol. Appl. 91 (2018) 228–235.

[19] V. Beachley, X. Wen, Effect of electrospinning parameters on the nanofiber diameter and length, Mater. Sci. Eng. C, Mater. Biol. Appl. 29 (2009) 663–668.

[20] N. Bhardwaj, S.C. Kundu, Electrospinning: a fascinating fiber fabrication technique, Biotechnol. Adv. 28 (2010) 325–347.

[21] T. Subbiah, G.S. Bhat, R.W. Tock, S. Parameswaran, S.S. Ramkumar, Electrospinning of nanofibers, J. Appl. Polym. Sci. 96 (2005) 557–569.

[22] R.E. Young, J. Graf, I. Miserocchi, R.M. Van Horn, M.B. Gordon, C.R. Anderson, L.S. Sefcik, Optimizing the alignment of thermoresponsive poly(N-isopropyl

[23] S.-W. Tsai, Y.-L. Yu, F.-Y. Hsu, Fabrication of polycaprolactone tubular scaffolds with an orthogonal-bilayer structure for smooth muscle cells, Mater. Sci. Eng. C 100 (2019) 308–314.

[24] S. Domaschke, M. Zündel, E. Mazza, A. Ehret, A 3D computational model of electrospun networks and its application to inform a reduced modelling approach, Int. J. Solid Struct. 158 (2018).

[25] Z.-C. Yao, J.-C. Wang, Z. Ahmad, J.-S. Li, M.-W. Chang, Fabrication of patterned three-dimensional micron scaled core-sheath architectures for drug patches, Mater. Sci. Eng. C 97 (2019) 776–783.

[26] S.H. Tan, R. Inai, M. Kotaki, S. Ramakrishna, Systematic parameter study for ultra-fine fiber fabrication via electrospinning process, Polymer 46 (2005) 6128–6134.

[27] S. Pisani, R. Dorati, B. Conti, T. Modena, G. Bruni, I. Genta, Design of copolymer PLA-PCL electrospun matrix for biomedical applications, React. Funct. Polym. 124 (2018) 77–89.

[28] K. Wang, H.-F. Wen, D. Yu, Y. Yang, D.-F. Zhang, Electrosprayed hydrophilic nanocomposites coated with shellac for colon-specific delayed drug delivery, Mater. Des. (2018) 143.

[29] K. Zhao, W. Wang, Y. Yang, K. Wang, D.-G. Yu, From Taylor cone to solid nanofiber in tri-axial electrospinning: size relationships, Res. Phys. 15 (2019) 102770.

[30] D. Yu, M. Wang, X. Li, X. Liu, L.-M. Zhu, S. Bligh, Multifluid Electrospinning for the Generation of Complex Nanostructures, Wiley Interdisciplinary Reviews: Nanomedicine and Nanobiotechnology, 2019e1601.

[31] M. Wang, T. Hai, Z. Feng, D.G. Yu, Y. Yang, S.A. Bligh, The relationships between the working fluids, process characteristics and products from the modified coaxial electrospinning of zein, Polymers (Basel) (2019) 11.

[32] H. Zhou, Z. Shi, X. Wan, H. Fang, D.G. Yu, X. Chen, P. Liu, The relationships between process parameters and polymeric nanofibers fabricated using a modified coaxial electrospinning, Nanomaterials (Basel) (2019) 9.

[33] S. Pisani, R. Dorati, E. Chiesa, I. Genta, T. Modena, G. Bruni, P. Grisoli, B. Conti, Release profile of gentamicin sulfate from polylactide-co-polycaprolactone electrospun nanofiber matrices, Pharmaceutics 11 (2019) 161.

[34] R. Dorati, S. Pisani, G. Maffeis, B. Conti, T. Modena, E. Chiesa, G. Bruni, U.M. Musazzi, I. Genta, Study on hydrophilicity and degradability of chitosan/polylactide-co-polycaprolactone nanofibre blend electrospun membrane, Carbohydr. Polym. 199 (2018) 150–160.

[35] R. Dorati, A. DeTrizio, I. Genta, P. Grisoli, A. Merelli, C. Tomasi, B. Conti, An experimental design approach to the preparation of pegylated polylactide-co-glicolide gentamicin loaded microparticles for local antibiotic delivery, Mater. Sci. Eng. C Mater. Biol. Appl. 58 (2016) 909–917.

[36] H.E. Abdelhakim, A. Coupe, C. Tuleu, M. Edirisinghe, D.Q.M. Craig, Electrospinning optimization of eudragit E PO with and without chlorpheniramine maleate using a design of experiment approach, Mol. Pharm. 16 (2019) 2557–2568.

[37] T. İnanç Horuz, K.B. Belibağlı, Production of electrospun gelatin nanofibers: an optimization study by using Taguchi's methodology, Mater. Res. Express 4 (2017) 015023.

[38] F. Gadala-Maria, F. Parsi, Measurement of fiber orientation in short-fiber composites using digital image processing, Polym. Compos. 14 (1993) 126–131.

[39] K. Nazari, P. Mehta, S. Arshad, S. Ahmed, E. Andriotis, N. Singh, O. Qutachi, M.-W. Chang, Z. Ahmad, Quality by design micro-engineering optimisation of NSAID-loaded electrospun fibrous patches, Pharmaceutics 12 (2019) 21.

[40] C. Ayres, G.L. Bowlin, S.C. Henderson, L. Taylor, J. Shultz, J. Alexander, T.A. Telemeco, D.G. Simpson, Modulation of anisotropy in electrospun tissue-engineering scaffolds: analysis of fiber alignment by the fast Fourier transform, Biomaterials 27 (2006) 5524–5534.

[41] Z. Puspoki, M. Storath, D. Sage, M. Unser, Transforms and operators for directional bioimage analysis: a survey, Adv. Anat. Embryol. Cell Biol. 219 (2016) 69–93.

[42] J.B. Lee, S.I. Jeong, M.S. Bae, D.H. Yang, D.N. Heo, C.H. Kim, E. Alsberg, I.K. Kwon, Highly porous electrospun nanofibers enhanced by ultrasonication for improved cellular infiltration, Tissue Eng. A 17 (2011) 2695–2702.

[43] X. Wang, B. Ding, B. Li, Biomimetic electrospun nanofibrous structures for tissue engineering, Mater. Today 16 (2013) 229–241.

[44] L. Chen, A. Al-shawk, C. Rea, H. Mazeh, X. Wu, W. Chen, Y. Li, W. Song, D. Markel, W. Ren, Preparation of electrospun nanofibers with desired microstructures using a programmed three-dimensional (3D) nanofiber collector, Mater. Sci. Eng. C 106 (2019) 110188.

[45] H. Wang, Aligned wet-electrospun starch fiber mats, Food Hydrocolloids 90 (2019) 113-117-2019 v.2090.

[46] M.K. Selatile, S.S. Ray, V. Ojijo, R. Sadiku, Correlations between fibre diameter, physical parameters, and the mechanical properties of randomly oriented biobased polylactide nanofibres, Fibers Polym. 20 (2019) 100–112.

[47] S. Kiros, S. Lin, M. Xing, K. Mequanint, Embryonic mesenchymal multipotent cell differentiation on electrospun biodegradable poly(ester amide) scaffolds for model vascular tissue fabrication, Ann. Biomed. Eng. 48 (2020) 980–991.

[48] S. Pisani, S. Croce, E. Chiesa, R. Dorati, E. Lenta, I. Genta, G. Bruni, S. Mauramati, A. Benazzo, L. Cobianchi, P. Morbini, L. Caliogna, M. Benazzo, M.A. Avanzini, B. Conti, Tissue engineered esophageal patch by mesenchymal stromal cells: optimization of electrospun patch engineering, Intrnl. J. Mol. Sci. 21 (2020).

[49] S.R. Jang, J. Kim, C. Park, C.s. Kim, The controlled design of electrospun PCL/silk/quercetin fibrous tubular scaffold using a modified wound coil collector and L-shaped ground design for neural repair, Mater. Sci. Eng. C 111 (2020) 110776.